Effect of length and thickness variations on the vibration of SWCNTs based on Flügge's shell model

Muzamal Hussain[1] ✉, *Muhammad Nawaz Naeem*[1], *Muhammad Taj*[2]

[1]*Department of Mathematics, Government College University Faisalabad, 38000 Faisalabad, Pakistan*
[2]*Department of Mathematics, University of Azad Jammu and Kashmir, Muzaffarabad, 1300, Azad Kashmir, Pakistan*
✉ *E-mail: muzamal45@gmail.com*

Published in Micro & Nano Letters; Received on 21st May 2019; Revised on 1st September 2019; Accepted on 10th October 2019

This work aims to investigate the vibration of the zigzag and chiral single-wall carbon nanotubes (SWCNTs) based on Flügge shell theory considering the clamped-simply supported, clamped-free, clamped-clamped and simply supported-simply supported end conditions. After developing the governing equation of the objective system, the wave propagation approach is implemented for the purpose of obtaining the frequency equation in the eigen form for vibration of the considered system. In addition, the applicability of this model for the analysis of vibration of carbon nanotube is examined with the effect of length and ratio of height-to-radius. To generate the fundamental natural frequencies of SWCNTs, computer software MATLAB engaged. The numerical results are validated with existing open text. Since the percentage of error is negligible, the model has been concluded as valid.

1. Introduction: Carbon nanotubes (CNTs) have a variety of applications because of their distinctive molecular structure and show unique electronic and mechanical properties because of their curvature. Nanotubes and micro-beams can be cited as one of the very applicable micro- and nano-structures in various systems, namely, sensing devices, communications and the quantum mechanics. The application of the tiny structures, specifically, CNTs in the sensors and actuators enforce the engineers to study vibrational properties of those structures experimentally and theoretically. In addition, they are utilised in different fields such as bio-engineering, tissue engineering, computer engineering, optics, energy and environmental systems. Therefore, their vibrational analysis is examined for successful application. Iijima [1] explored CNTs in 1991.

Some researchers [2–7] used the aspect ratio (5–100 nm) with higher frequencies (THz$\sim 10^{17}$). In material strength analysis, the application of CNTs has a vast field [1, 5, 8, 9]. Gigault *et al.* [10] carried out the experiment on the SWCNT size characteristics with aspect ratio from <500 up to 2000 nm using Raman and scanning electron microscopy techniques. Leung and Kuang [11] conducted a numerical study of the axial compression and external hydrostatic pressure of multi-walled CNTs (MWCNTs) based on Flügge's theory of the elastic stability of thin cylindrical shells. Bocko and Lengvarský [4] studied the natural frequency versus length ($L = 10$–100 nm) with varying two distinct diameters ($D = 1356$ and 2034 nm) using non-local theory. Wang *et al.* [12] applied Flügge shell equations of elastic shells to investigate the vibration of MCWNTs. The natural frequencies and mode shape are calculated for MWCNTs with radii 0.65 and 5 nm, respectively. Natsuki *et al.* [13] proposed the vibration analysis of single- and double-walled CNTs using Flügge shell model. The frequencies are analysed and investigated to find the effect of vibrational modes and nanotube parameter.

Hussain and Naeem [5] studied the vibrations of armchair SWCNTs using wave propagation approach (WPA). They investigated the natural frequency versus length ($L = 10$–100 nm) with varying three distinct radii ($R = 678$, 1356 and 2034 nm). Moreover, Wang and Zhang [14] studied the vibration frequency spectra to extract the bending and torsion stiffness for SWCNTs by employing the Flügge's shell model. It was concluded that with the well-defined thickness, a shell model of SWCNTs can be established. Alibeigloo and Shaban [15] investigated the frequencies of SWCNTs using the three-dimensional elastic theory and concluded that the frequencies increases by increasing the thickness-to-radius ratio ($h/R = 0.02$–0.1) keeping the length ($L = 5$ nm). Selim [16] studied the torsional vibration of SWCNTs in multilayer shells and the Flügge shell model was proposed for vibration of CNTs with additional phase velocity subject to initial compressive stress. Ghavanloo and Fazelzadeh [17, 18] exhibited the remarkable mechanical phenomena on vibration of SWCNTs. In this study, an isotropic elastic shell model is developed by using the Flügge's shell theory. Recently, many researchers used Flügge shell model to investigate the vibration of CNTs [19–21]. Moreover, many researchers used different models through computer computations in open text [8, 12, 15, 19] to calculate the overall vibrational behaviour of CNTs. Due to the exactness of this approach, some researchers have been used for the vibration of CNT [12, 13, 16, 17, 18]. To the best of knowledge, element formulations for SWCNTs using WPA with different theories have not been explicitly reported in the open literature. In addition, the main advantage of the novel method based on WPA is that it is a very simple method and the advantages are to explore a new horizon for examining the overall vibration analysis of SWCNTs and proposed method converges faster than earlier computations such as beam models and molecular dynamics simulations. According to this simulation, the percentage and statistical error have been reduced within the acceptable range and another better option to escape from mathematical rigors than earlier computations as beam model (BM) and Timoshenko beam model (TBM) [8, 13]. The results gained here are compared with earlier models. We are investigating the influence of length and ratio of height-to-radius for zigzag and chiral SWCNTs on the vibration fundamental natural frequencies (FNFs), which is our particular motive.

The researchers recommended the beam theories [8, 13] to investigate the behaviour of nanostructure. These models are also having drawbacks and the other theories/simulation like beam theories and molecular dynamic simulation cannot be investigated by the cross-sectional deformation and geometrical parameters (thickness and height-to-radius). Shells theory of Flügge is discussed in this Letter for modelling with cross-sectional deformation of SWCNTs. Appropriate theory are performed to find out the complex behaviour of nanostructures. The most important geometrical parameters are basically obtained from numerical studies of shell theory and this parameter provides a platform for the

correctness of the results. Furthermore, it is suggested that the proposed theory might be a reliable indicator of the tube thickness and length in the SWCNT. These results would be beneficial for determining the optimum structure of SWCNTs. The thicknesses can then be used to provide quantitative values for the amount of SWCNT material added to the current collectors.

2. Theoretical formation: Due to geometrical shapes, SWCNTs and cylindrical shells are observed similar in structure. So for studying the vibration of SWCNTs, the equation of motion of cylindrical shells is used. Moreover, Fig. 1*a* shows the orientation of the graphene sheet as, nanotubes become zigzag, if $m = 0$ and the nanotubes are chiral if $n \neq m$, respectively. Here, vibration frequencies zigzag indices (12, 0), (14, 0), (19, 0) and (8, 3), (10, 2), (14, 5) for chiral SWCNTs, respectively, have been performed using Flügge shell model based on WPA. The results have been given only for different eigen-frequencies for radius 678, 1356 and 2034 nm for zigzag and chiral with length, and also ratio of thickness-to-radius for these tubes. Figs. 1*a* and *b* shows geometrical variation of indices of zigzag and chiral SWCNTs.

A SWCNT with geometrical parameters length, mean radius and thickness denoted as L, R and h, respectively, is shown in Fig. 2. Young's modulus, Poisson's ratio and mass density are denoted by their material quantities as E, ν and ρ, respectively. Suppose that the displacement functions u_1, u_2, u_3 are in the direction of axial, tangential and transverse, respectively. For executing the vibration of CNTs, a set of partial differential equations (PDEs) [14] containing displacement functions is written as: $\frac{\partial^2\alpha}{\partial\phi^2} + \left(\frac{1-\nu}{2R^2}\right)\frac{\partial^2\alpha}{\partial\psi^2} + \left(\frac{1+\nu}{2R}\right)\frac{\partial^2\beta}{\partial\phi\partial\psi} - \left(\frac{\nu}{R}\right)\frac{\partial\gamma}{\partial\phi} = \frac{\rho}{K_{\text{extension}}}\frac{\partial^2\alpha}{\partial t^2}$

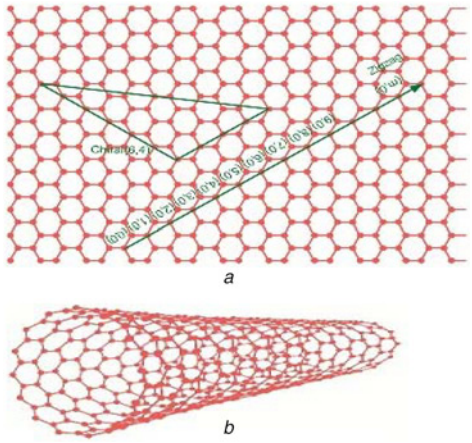

Fig. 1 *Schema of hexagonal Lattice*
a Graphene sheet with indices
b SWCNTs

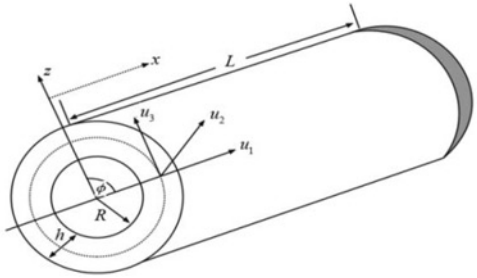

Fig. 2 *Geometry of SWCNTs*

$$
\begin{aligned}
&\frac{1+\nu}{2R}\frac{\partial^2\alpha}{\partial\phi\partial\psi} + \frac{1-\nu}{2}\frac{\partial^2\beta}{\partial\phi^2} + \frac{1}{R^2}\frac{\partial^2\beta}{\partial\psi^2} - \frac{1}{R^2}\frac{\partial\gamma}{\partial\psi} \\
&\quad + \frac{1}{R^2}K_1\left(K_2\frac{\partial^2\beta}{\partial\phi^2} + \frac{\partial^2\beta}{R^2\partial\psi^2}\right) \\
&\quad + \frac{1}{R^2}K_1\left(\frac{1}{R^2}\frac{\partial^3\gamma}{\partial\psi^3} + (K_2+\nu)\frac{\partial^3\gamma}{\partial\phi^2\partial\psi}\right) \\
&= \frac{\rho}{K_{\text{extension}}}\frac{\partial^2\beta}{\partial t^2}\frac{\nu}{R}\frac{\partial\alpha}{\partial\phi} + \frac{1}{R^2}\frac{\partial\beta}{\partial\psi} - \frac{\gamma}{R^2} \\
&\quad - \frac{1}{R^2}K_1\left(R^2\frac{\partial^4\gamma}{\partial\phi^4} + 2(K_2+\nu)\frac{\partial^4\gamma}{\partial\phi^2\partial\psi^2} + \frac{1}{R^2}\frac{\partial^4\gamma}{\partial\psi^4}\right) \\
&\quad - \frac{1}{R^2}K_1\left((2K_2+\nu)\frac{\partial^3\beta}{\partial\phi^2\partial\psi} + \frac{1}{R^2}\frac{\partial^3\beta}{\partial\psi^3}\right) = \frac{\rho}{K_{\text{extension}}}\frac{\partial^2\gamma}{\partial t^2}
\end{aligned}
\tag{1}
$$

where $K_1 = D_{\text{bending}}/K_{\text{extension}}$, $K_2 = D_{\text{torsion}}/D_{\text{bending}}$ and the in-plane, torsional, bending and shear stiffness are designated by $K_{\text{extension}}$, D_{torsion}, D_{bending} and K_{shear}, respectively, G denotes the shear modulus. These parameters are preserved as independent parameters termed mathematically as

$$
K_{\text{extension}} = \frac{Eh}{1-\nu^2},\ K_{\text{shear}} = Gh,\ D_{\text{bending}} = \frac{Eh^3}{12(1-\nu^2)}
$$

$$
D_{\text{torsion}} = \frac{Gh^3}{12} \text{ and } G = \frac{E}{2(1+\nu)}
$$

Above quantities have a unique relationship as follows:

$$
\frac{D_{\text{bending}}}{K_{\text{extension}}} = \frac{D_{\text{torsion}}}{K_{\text{shear}}} = \frac{h^2}{12}
$$

3. Wave propagation approach: WPA is used to study the vibrational behaviour of SWCNTs. Before this work, current approach was successfully used for vibration, and buckling analysis of cylindrical shell [5, 9, 13, 22, 23] was used to discretise the governing equation of motion. The coordinate system ϕ, ψ, t is designated for axial, circumferential and time variable. The following relations for displacement functions are assumed as

$$
\begin{aligned}
\alpha(\phi, \psi, t) &= \mathrm{e}^{i\omega t}\cos n\psi A_\iota p(\phi) \\
\beta(\phi, \psi, t) &= \mathrm{e}^{i\omega t}\sin n\psi B_\iota q(\phi) \\
\gamma(\phi, \psi, t) &= \mathrm{e}^{i\omega t}\cos n\psi C_\iota S(\phi)
\end{aligned}
\tag{2}
$$

where three vibrational amplitude coefficients denotes, respectively, the direction of axial, circumferential and radial. Here ω, m, n are denoted by angular frequency, axial half and the circumferential wave numbers, respectively. A_ι, B_ι and C_ι are taken as the displacement amplitudes in x, θ and z directions and the angular frequency and circumferential wave number are represented by ω and n, respectively. $f = \omega/2\pi$ is the FNF formula. The space and temporal variables are separated by using product method for PDEs. Also, the complex exponential function is specified for the axial modal function denoted by $p(\phi)$, $q(\phi)$ and $s(\phi)$ as

$$
p(\phi) = q(\phi) = s(\phi) = \mathrm{e}^{-iJ_\delta\phi} \tag{3}
$$

The deformation functions α, β, γ have been written as in the form of complex exponential function involving k_m, which is axial wave number related with an end condition [14]. Now the expressions for α, β, γ given in (2), along with their partial derivatives are substituted into (1). Also making substitutions from modal expressions for $p(\phi)$, $q(\phi)$, $s(\phi)$ and their respective derivatives in the

doi: 10.1049/mnl.2019.0309

system of algebraic linear equations is obtained

$$\begin{aligned}
&\left[J_\delta^2 + y^2\frac{1-v}{2R^2}\right]A_\iota + \left[iJ_\delta y\right]\frac{1+v}{2R}B_\iota - \frac{v}{R}iJ_\delta C_\iota = \omega^2\frac{\rho}{K_{\text{extension}}}A_\iota \\
&\left[-y\frac{1+v}{2R}iJ_\delta\right]A_\iota - \left[-\frac{1+v}{2}J_\delta^2 - \frac{y^2}{R^2} - \frac{K_1}{R^2}\left\{K_2J_\delta^2 + \frac{y^2}{R^2}\right\}\right]B_\iota \\
&\quad - \left[\frac{y}{R^2} + \frac{K_1}{R^2}\left\{\frac{y^3}{R^2} + (K_2+v)yJ_\delta^2\right\}\right]C_\iota = \frac{\rho}{K_{\text{extension}}}\omega^2 B_\iota \\
&\frac{v}{R}iJ_\delta A_\iota - \left[\frac{y}{R^2} + \frac{K_1}{R^2}\left\{(2K_2+v)J_\delta^2 y + \frac{y^3}{R^2}\right\}\right]B_\iota \\
&\quad - \left[-\frac{1}{R^2} - \frac{K_1}{R^2}\left\{R^2J_\delta^4 + 2(K_2+v)J_\delta^2y^2 + \frac{y^4}{R^2}\right\}\right]C_\iota \\
&= \frac{\rho}{K_{\text{extension}}}\omega^2 C_\iota
\end{aligned} \tag{4}$$

The matrix equation to represent the frequencies, after the arrangement of terms can be written as

$$\begin{bmatrix} d_{11} & d_{12} & d_{13} \\ d_{21} & d_{22} & d_{23} \\ d_{31} & d_{32} & d_{33} \end{bmatrix}\begin{pmatrix} A_\iota \\ B_\iota \\ C_\iota \end{pmatrix} = \frac{\rho}{K_{\text{extension}}}\omega^2\begin{bmatrix} 1 & 0 & 0 \\ 0 & 1 & 0 \\ 0 & 0 & 1 \end{bmatrix}\begin{pmatrix} A_\iota \\ B_\iota \\ C_\iota \end{pmatrix} \tag{5}$$

where the matrix elements $d_{ij} = 1 \le i,\ j \le 3$ are specified as follows:

$$\begin{aligned}
&d_{11} = -\frac{v}{R}ik_m\alpha_m - \frac{1-v}{2R^2},\ d_{12} = \frac{1+v}{2R}nik_m,\ d_{13} = -\frac{v}{R}ik_m \\
&d_{21} = \frac{1+v}{2R}nik_m,\ d_{22} = -\frac{1-v}{2}k_m^2 - \frac{n^2}{R^2} - \frac{K_1}{R^2}\left(K_2k_m^2 + \frac{n^2}{R^2}\right), \\
&d_{23} = \frac{n}{R^2} + \frac{K_1}{R^2}\left(\frac{n^3}{R^2} + (K_2+v)nk_m^2\right) \\
&d_{31} = -\frac{v}{R}ik_m,\ d_{32} = \frac{n}{R^2} - \frac{K_1}{R^2}\left(-(2K_2+v)nk_m^2 - \frac{n^3}{R^2}\right), \\
&d_{33} = -\frac{1}{R^2} - \frac{K_1}{R^2}\left((R^2k_m^4) + 2(K_2+v)n^2k_m^2 + \frac{n^4}{R^2}\right)
\end{aligned}$$

For vibrating CNT, the axial wave number k_m is related to an end condition specified at the CNT end. This is the actual characteristics for adapting the WPA here.

4. Result and discussion: The obtained results for the different boundary conditions (BCs) are likewise: simply supported-simply supported (SS-SS), clamped-clamped (C-C), clamped-free (C-F) and clamped-simply supported (C-S) for zigzag and chiral SWCNTs are parametrically studied in this part. The results for length and ratio of thickness-to-radius are presented versus fundamental frequencies f (THz × 10^4) and f (THz × 10^6), respectively. For example, the reported effective thickness of SWCNTs ranges from 0.0612 to 0.69 nm [5, 8, 9] whose magnitude difference is more than an order. In most of the previous studies, the value of $K_{\text{extension}}$ is obtained and lies in the range of 330–363 J/m^2 [5, 9] and Poisson's ratio v arises from 0.14 to 0.34. The frequency can be controlled by varying several parameters. The graphical behaviour of frequencies versus aspect ratio/length-to-diameter ratio of [4, 7] is same and shows a good validity. Figs. 3–5 show the variation of frequencies versus length of zigzag (12, 0), (14, 0) and (19, 0) with various BCs. Particularly, the natural frequencies corresponding to length (L = 10 nm) for zigzag indices (12, 0), (14, 0), (19, 0) are 14.102, 16.358, 21.999, for the C-C end condition, 13.820, 16.076, 21.717, for the C-SS end condition, 13.538, 15.794, 21.435, for the SS-SS end condition, and 12.974, 15.230, 20.871, for the C-F support condition, respectively. Similarly, the frequencies corresponding to length (L = 100 nm) for zigzag indices (12, 0), (14, 0), (19, 0) are 1.4102, 1.6358, 2.1999, for the C-C end condition, 1.3820, 1.6076, 2.1717, for the C-SS, 1.3538, 1.5794, 2.1435, for the SS-SS end condition, and 1.2974, 1.5230, 2.0871, for the C-F end condition, respectively. It shows that the natural frequencies decreased as L is enhanced by these BCs. It is observed that there is minute difference with different BCs and frequencies of C-F are lower than other BCs. It is can be seen from Figs. 3–5 that the FNFs values of zigzag (12, 0) are lower than those of FNFs of (14, 0) and (19, 0). Figs. 6–8 show the variation of frequencies versus length of chiral (8, 3), (10, 2)

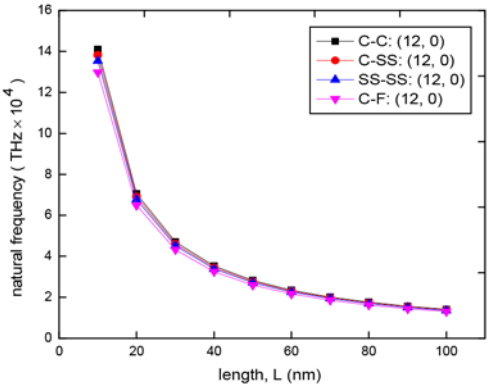

Fig. 3 *FNFs versus length for zigzag SWCNTs (12, 0) with R = 678 nm and h = 0.1 nm*

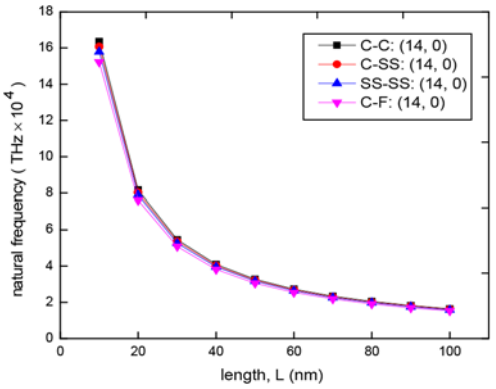

Fig. 4 *FNFs versus length for zigzag tube (14, 0) with R = 1356 nm and h = 0.1 nm*

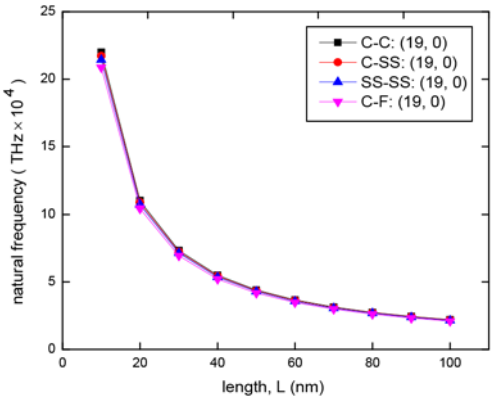

Fig. 5 *FNFs versus length for zigzag SWCNTs (19, 0) with R = 2034nm and h = 0.1 nm*

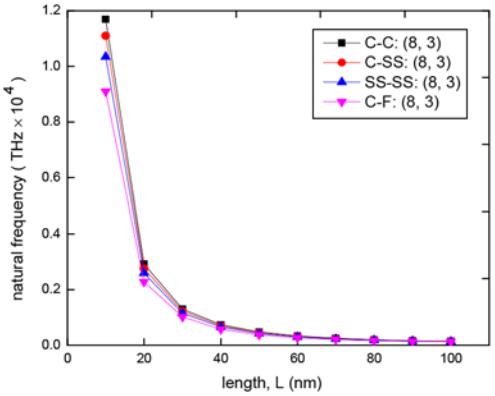

Fig. 6 *FNFs versus length for chiral tube (14, 0) with R = 678 nm and h = 0.1 nm*

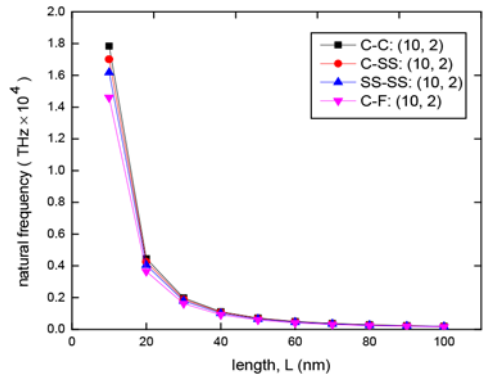

Fig. 7 *FNFs versus length for chiral tube (10, 2) with R = 1356 nm and h = 0.1 nm*

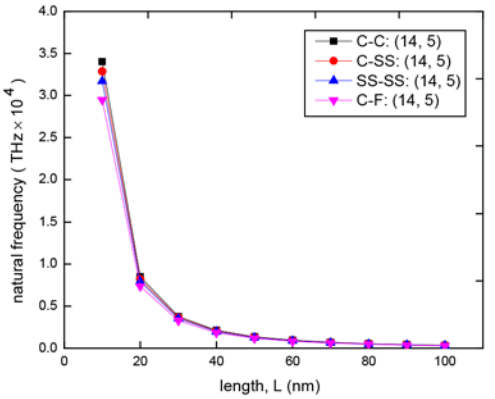

Fig. 8 *FNFs versus length for chiral tube (14, 5) with R = 2034nm and h = 0.1 nm*

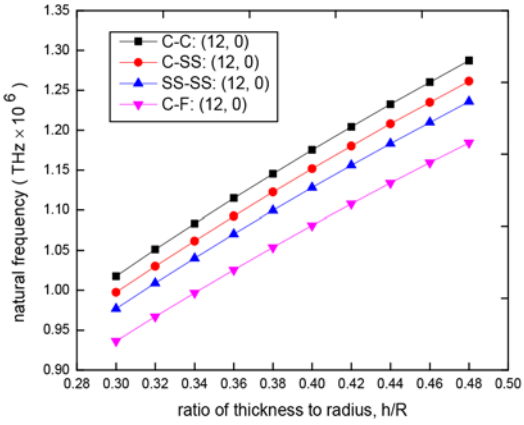

Fig. 9 *FNFs versus h/R for zigzag tube (12, 0) with L = 2.4 nm*

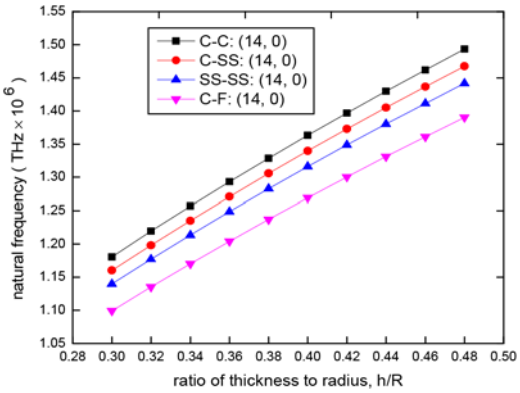

Fig. 10 *FNFs versus h/R for zigzag tube (14, 0) L = 2.4 nm*

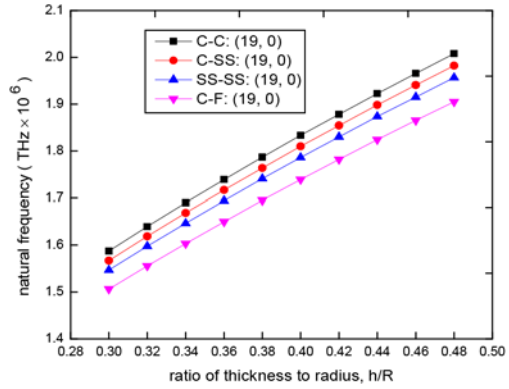

Fig. 11 *FNFs versus h/R for zigzag tube (19, 0) with L = 2.4 nm*

and (14, 5) with various BCs. Particularly, the natural frequencies corresponding to length ($L = 10$ nm) for chiral indices (8, 3), (10, 2), (14, 5) are 1.169, 1.784, 3.401, for the C-C end condition, 1.1101, 1.700, 3.285, for the C-SS end condition, 1.035, 1.618, 3.171, for the SS-SS end condition, and 0.910, 1.460, 2.948, for the C-F end condition, respectively.

Similarly, the natural frequencies corresponding to length ($L = 100$ nm) for chiral indices (8, 3), (10, 2), (14, 5) are 0.0143, 0.0196, 0.0350, for the C-C end condition, 0.0137, 0.0189, 0.0339, for the C-SS end condition, 0.0132, 0.0181,0.0328, for the SS-SS end condition, and 0.123, 0.0167, 0.0306, for the C-F end condition, respectively. For all BCs, the frequencies fall down, then, become parallel and, after that, seem linear and there is minute difference between them. It can be seen from these figures that the FNF values of chiral (14, 5) are higher than those of (8, 3) and (10, 2). The frequencies are more visible as compared to zigzag case. It is also concluded that the frequency increases with increasing tube radius.

This increase is more prominent especially for higher radius and significant effect of radius can be observed over natural frequencies. Figs. 9–11 show the variation of frequencies versus ratio of height-to-radius of zigzag (12, 0), (14, 0) and (19, 0), with various BCs. Particularly, the natural frequencies corresponding to height-to-radius ratio ($h/R = 0.30$) for end condition

doi: 10.1049/mnl.2019.0309

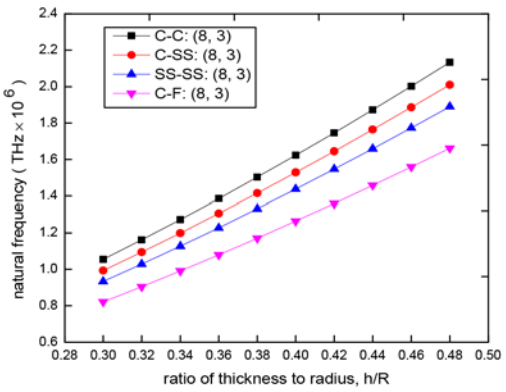

Fig. 12 *FNFs versus h/R for chiral tube (8, 3) with L = 2.4 nm*

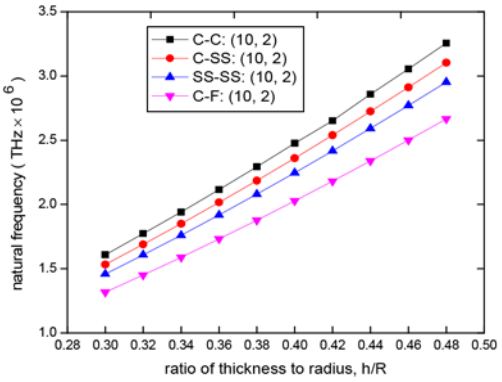

Fig. 13 *FNFs versus h/R for chiral tube (10, 2) with L = 2.4 nm*

C-C (12, 0), (14, 0), (19, 0) are 1.0177, 1.1806, 1.5876, for end condition C-S (12, 0), (14, 0), (19, 0) are 0.9974, 1.1602, 1.5673, for SS-SS (12, 0), (14, 0), (19, 0) are 0.9770, 1.1398, 1.5469, and for end condition C-F (12, 0), (14, 0), (19, 0) are 0.9363, 1.0991, 1.5062, respectively. Similarly, the natural frequencies corresponding to thickness-to-radius ratio ($h/R = 0.48$) for end condition C-C (12, 0), (14, 0), (19, 0) are 1.2873, 1.4933, 2.008, for end condition C-S (12, 0), (14, 0), (19, 0) are 1.2616, 1.4675, 1.9824, for SS-SS (12, 0), (14, 0), (19, 0) are 1.2358, 1.4418, 1.9567, and for C-F (12, 0), (14, 0), (19, 0) are 1.1843, 1.3903, 1.905, respectively. For these BCs, on increasing the thickness-to-radius ratio h/R, the frequencies also increase. At h/R (= 0.30 to 0.48), all the frequencies are parallel. In these figures, it can be seen that the gap between the C-C, C-S, SS-SS is smaller than that of CF BC. It can be seen that the FNFs of zigzag (14, 0) are between the frequencies of (12, 0) and (19, 0). Figs. 12–14 show the variation of frequencies versus ratio of height-to-radius of chiral (8, 3), (10, 2) and (14, 5) with various BCs. Particularly, the FNFs at $h/R = 0.30$ for end condition C-C = (8, 3) f ~1.0544, (10, 2) f ~1.6089, (14, 5) f ~3.0683, for C-S = (8, 3) f ~0.9933, (10, 2) f ~1.5332, (14, 5) f ~2.9634, for SS-SS = (8, 3) f ~0.9340, (10, 2) f ~1.4593, (14, 5) f ~2.8609, and for end condition C-F = (8, 3) f ~0.8208, (10, 2) f ~1.3171, (14, 5) f ~2.6596, respectively.

Similarly, the natural frequencies corresponding to ratio of thickness-to-radius ($h/R = 0.48$) for end condition C-C = (8, 3) f ~2.1339, (10, 2) f ~3.2562, (14, 5) f ~6.2097, for end condition C-S = (8, 3) f ~2.0102, (10, 2) f ~3.1030, (14, 5) f ~5.9974, for SS-SS = (8, 3) f ~1.8902, (10, 2) f ~2.9535, (14, 5) f ~5.7889, and for C-F = (8, 3) f ~1.6613, (10, 2) f ~2.6655, (14, 5) f ~5.3827, respectively. As h/R is enhanced for these BCs, the frequencies go up. At h/R (= 0.30–0.48), all the frequencies are parallel. It can be seen that the C-S, SS-SS are sandwiched between C-C and C-F BCs. The FNFs of (14, 5) are higher than those of (8, 3) and (10, 2).

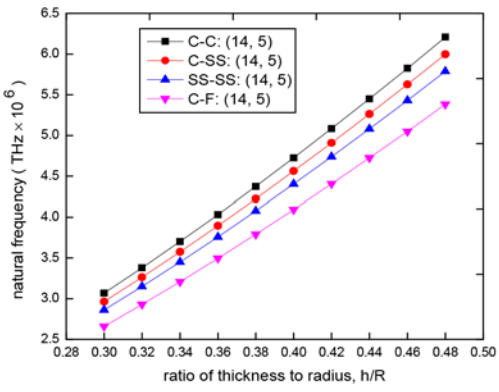

Fig. 14 *FNFs versus h/R for chiral tube (14, 5) with L = 2.4 nm*

5. Conclusions: The discussion in this Letter shows the vibration of zigzag and chiral SWCNTs based on WPA with different end conditions. Frequency spectra of zigzag (12, 0), (14, 0), (19, 0) and chiral (8, 3), (10, 2), (14, 5) SWCNTs for length and ratio of thickness-to-radius have been investigated. The length with different BCs has been carried out for three different values of radius and noted the frequency values for each case of zigzag and chiral SWCNTS. At higher value of length, the frequencies are diminished. On the other hand, the phenomena of frequency versus height-to-radius ratio are a counterpart of length. When the ratio of height-to-radius increases, the FNFs also increase for all sort of SWCNTs. The frequency values of zigzag are higher than that of chiral. Throughout the computation, it is observed that the frequency behaviour for the BC follows as: C-C frequency curves are higher than that of C-SS, SS-SS and C-F curves, respectively. From the above discussion, it is concluded that end conditions have a notable effect on the vibration of SWCNTs. The investigation presented may be helpful in the application of MWCNTs such as high-frequency oscillators and mechanical sensors.

6 References

[1] Iijima S.: 'Helical microtubules of graphitic carbon', *Nature'*, 1991, **345**, pp. 56–58

[2] Imani Yengejeh S., Akbar Zadeh M., Öchsner A.: '75 numerical modeling of eigenmodes and eigenfrequencies of hetero-junction carbon nanotubes with pentagon–heptagon pair defects', *Comput. Mater. Sci.*, 2014, **92**, pp. 76–83

[3] Lü J., Chen H., Lü P., *ET AL.*: 'Research of natural frequency of single-walled carbon nanotube', *Chin. J. Chem. 95 Phys.*, 2007, **20**, p. 525

[4] Bocko J., Lengvarský P.: 'Vibration of single-walled carbon nanotubes by using nonlocal theory', *Am. J. Mech. Eng.*, 2014, **2**, pp. 195–198

[5] Hussain M., Naeem M.N.: 'Vibration analysis of single-walled carbon nanotubes using wave propagation approach', *Mech. Sci.*, 2017, **8**, (1), pp. 155–164

[6] Swain A., Roy T., Nanda B.K.: 'Vibration behavior of single-walled carbon nanotube using finite element', *Int. J. Theor. Appl. Res. Mech. Eng.*, 2013, **2**, pp. 129–133

[7] Zhang Y.Y., Wang C.M., Tan V.B.C.: 'Assessment of timoshenko beam models for vibrational behavior of single-walled carbon nanotubes using molecular dynamics', *Adv. Appl. Math. Mech.*, 2009, **1**, (1), pp. 89–106

[8] Yakobson B.I., Brabec C.J., Bernholc J.: 'Nanomechanics of carbon tubes: instabilities beyond linear response', *Phys. Rev. Lett.*, 1996, **76**, (14), pp. 2511–2514

[9] Hussain M., Naeem M. N., Shahzad A., *ET AL.*: 'Vibrational behavior of single-walled carbon nanotubes based on cylindrical shell model using wave propagation approach', *AIP. Adv.*, 2017, **7**, (4), p. 045114

[10] Gigault J., Le Hécho I., Dubascoux S., *ET AL.*: 'Single walled carbon nanotube length determination by asymmetrical-flow field-flow

fractionation hyphenated to multi-angle laser-light scattering', *J. Chromatogr., A*, 2010, **1217**, (50), pp. 7891–7897
[11] Leung A.Y.T., Kuang J.L.: 'Nanomechanics of a multi-walled carbon nanotube via flugge's theory of a composite cylindrical lattice shell', *Phys. Rev. B*, 2005, **71**, (16), p. 165415
[12] Wang C. Y., Ru C. Q., Mioduchowski A.: 'Free vibration of multiwall carbon nanotubes', *J. Appl. Phys.*, 2005, **97**, (11), pp. 1–11
[13] Natsuki T., Endo M., Tsuda H.: 'Vibration analysis of embedded carbon nanotubes using wave propagation approach', *J. Appl. Phys.*, 2006, **99**, (3), p. 034311
[14] Wang C.Y., Zhang L.C.: 'Modelling the free vibration of single-walled carbon nanotubes'. 5th Australasian Congress on Applied Mechanics (ACAM), Brisbane, Australia, 2007, 1, Engineers Australia
[15] Alibeigloo A., Shaban M.: 'Free vibration analysis of carbon nanotubes by using three-dimensional theory of elasticity', *Acta Mech.*, 2013, **224**, (7), pp. 1415–1427
[16] Selim M.M.: 'Torsional vibration of carbon nanotubes under initial compression stress', *Braz. J. Phys.*, 2010, **40**, (3), pp. 283–287
[17] Ghavanloo E., Fazelzadeh S. A.: 'Vibration characteristics of single-walled carbon nanotubes based on an anisotropic elastic shell model including chirality effect', *Appl. Math. Modell.*, 2012, **36**, (10), pp. 4988–5000
[18] Harris P.J.F.: 'Carbon nanotube science synthesis, properties and applications' (Wiley-VCH Verlag GmbH & Co. KGaA, Germany, 2009)
[19] Ansari R., Arash B.: 'Nonlocal Flügge shell model for vibrations of double-walled carbon nanotubes with different boundary conditions', *J. Appl. Mech.*, 2013, **80**, (2), p. 021006
[20] Ansari R., Rouhi H.: 'Nonlocal flugge shell model for the axial buckling of single-walled carbon nanotubes: an analytical approach', *Int. J. Nano. Dimens.*, 2015, **6**, (5), pp. 453–462
[21] Rouhi H., Bazdid-Vahdati M., Ansari R.: 'Rayleigh-Ritz vibrational analysis of multiwalled carbon nanotubes based on the nonlocal Flügge shell theory', *J. Compos.*, 2015, **2015**, pp. 1–11, doi:10.1155/2015/750392
[22] Hussain M., Naeem M. N.: 'Vibration of single-walled carbon nanotubes based on Donnell shell theory using wave propagation approach', in Kyvas G.Z., Mitropoulo A.C. [EDs.]: Novel Nanomaterials – Synthesis and Applications (IntechOpen, UK, 2018)
[23] Hussain M., Naeem M.N., Isvandzibaei M.R.: 'Effect of Winkler and Pasternak elastic foundation on the vibration of rotating functionally graded material cylindrical shell', *Proc. Inst. Mech. Eng., C: J. Mech. Eng. Sci.*, 2018, **232**, (24), pp. 4564–4577

doi: 10.1049/mnl.2019.0309